Multi-Frequency Polarimetric SAR Data Analysis for Crop Type Classification Using Random Forest

Hariharan, Siddharth; Mandal, Dipankar; Tirodkar, Siddhesh; Kumar, Vineet; Bhattacharya, Avik

DOI
10.1007/978-3-031-21225-3_8

Publication date
2022

Document Version
Final published version

Published in
Synthetic Aperture Radar (SAR) Data Applications

Citation (APA)
Hariharan, S., Mandal, D., Tirodkar, S., Kumar, V., & Bhattacharya, A. (2022). Multi-Frequency Polarimetric SAR Data Analysis for Crop Type Classification Using Random Forest. In M. Rysz, A. Tsokas, K. M. Dipple, K. L. Fair, & P. M. Pardalos (Eds.), *Synthetic Aperture Radar (SAR) Data Applications* (pp. 195-217). (Springer Optimization and Its Applications; Vol. 199). Springer. https://doi.org/10.1007/978-3-031-21225-3_8

Multi-Frequency Polarimetric SAR Data Analysis for Crop Type Classification Using Random Forest

Siddharth Hariharan, Dipankar Mandal, Siddhesh Tirodkar, Vineet Kumar, and Avik Bhattacharya

1 Introduction

Classification of crops is an efficient way for managing agricultural areas and monitoring yield. One of the successful ways of doing this is the use of Synthetic Aperture Radar (SAR) data as recognized widely in the last two decades. The potential of SAR for crop classification is significant since radar backscattering is sensitive to the dielectric properties of the vegetation and the soil, plant geometry, and surface roughness. Additionally SAR systems can operate efficiently under all weather conditions making them ideal for crop classification. Crop classification

S. Hariharan
Computer Engineering Department, TPCT's Terna Engineering College, Mumbai, India
e-mail: siddharthkalpagam@ternaengg.ac.in

D. Mandal (✉)
Kansas State University, Manhattan, KS, USA
e-mail: dmandal@ksu.edu

S. Tirodkar
Geophysical and Multiphase Flows Laboratory, IDP in Climate Studies, Indian Institute of Technology Bombay, Mumbai, India
e-mail: siddhesh.t@iitb.ac.in

V. Kumar
Department of Water Resources, Delft University of Technology, Delft, The Netherlands
e-mail: V.Kumar-1@tudelft.nl

A. Bhattacharya
Microwave Remote Sensing Lab, Centre of Studies in Resources Engineering, Indian Institute of Technology Bombay, Mumbai, India
e-mail: avikb@csre.iitb.ac.in

M. Rysz et al. (eds.), *Synthetic Aperture Radar (SAR) Data Applications*, Springer Optimization and Its Applications 199, https://doi.org/10.1007/978-3-031-21225-3_8

using SAR data has produced admissible accuracies in literature [4, 13, 15, 25, 29–31, 43, 48, 56].

Multi-frequency polarimetric SAR analysis of crops is even more useful since the different depths of penetration of the EM wave at various frequencies give unique information about the crop structure, vegetation water content, and biomass [44]. Multi-frequency data, available by airborne SAR systems like the AIRSAR, indicate interesting crop classification results [19, 24, 34] due to differences in multi-frequency polarimetric parameters associated with different plant geometries. Rao et al. [50] indicated monotonic decrease in co-pol phase difference (ϕ_{HH-VV}) over corn fields at multi-frequency (P-, L-, C-band) polarimetric AIRSAR data. At higher frequencies, radar backscatter return is more correlated with heads and fruiting part, while they are better correlated with wet biomass and foliar area at lower frequencies [27].

With the availability of multi-frequency SAR data from space borne platforms (multi-sensor), crop classification studies have received much attention from remote sensing community [47, 48]. These studies indicated that high biomass crops (e.g., corn) were well classified using the low frequency data, while higher frequency data were needed to accurately classify low biomass crops. New generation SAR system promises better availability of multi-frequency data from Copernicus Sentinel-1 program (C-band), RADARSAT Constellation Mission (C-band), SAOCOM-1A/B (L-band), TerraSAR-X (X-band), and upcoming ROSE-L, Biomass, and NASA-ISRO SAR (NISAR L- and S-band) missions. Nevertheless, diversity in frequency is still only attainable by integrating data from multiple platforms and enabling enhanced crop characterization capabilities by the synergy among these cross platforms [6, 17, 44, 52].

The major features used in crop classification experiments are confined to backscatter intensities at different polarization channels (HH, VV, and HV or VH) [14, 41, 46, 53]. Additional information about the physical nature of the crops can be obtained by generating the target decomposition polarimetric parameters from fully polarimetric SAR data. Moreover, the ratios of individual backscatter coefficients convey additional target scattering information [28, 45]. In addition to the individual backscattering coefficients, polarimetric target decomposition parameters obtained from both model based and eigenvalue-eigenvector based polarimetric parameters [9, 60, 65] can better characterize different crops.

Identifying relevant and important polarimetric parameters is an integral part of machine learning studies. Many machine learning techniques employ parameter selection to form subsets resulting in dimensionality reduction. Some of the machine learning techniques used for crop classification using SAR data are neural network classifier [8], maximum likelihood classifier [33], Wishart classification [33, 55], Support Vector Machines (SVM) [39], decision-tree classifier [47].

Among different classifiers, the Random Forest (RF) is gaining much attention for land cover classification over agricultural areas [10, 11, 13, 22, 36, 38, 42, 58, 64]. RF also provides a parameter subset as a part of its classification technique. RF additionally handles the diverse dynamic ranges of the polarimetric parameters and it does not require parameter scaling or normalization. This provides an added

advantage over other techniques since the polarimetric parameters used in crop classification have varied ranges. In this work, we use polarimetric target decomposition parameters obtained from both model based and eigenvalue-eigenvector based polarimetric parameters in addition to the individual backscattering coefficient parameters in a RF classifier.

The rest of this chapter is organized in the following order: Sect. 2 briefly describes the study area and datasets used. Section 3 explains in detail the methodology of multi-frequency crop classification used in this study. Section 4 discusses the results and their subsequent observations and interpretations in depth; and finally, this chapter is succinctly summarized and concluded in Sect. 5.

2 Study Area and Dataset

We conducted the study over the international agricultural super-site at Flevoland area in The Netherlands (Fig. 1). The test site is bounded between 52.266605°N, 5.648201°E (upper left coordinate) and 52.326725°N, 5.441733°E (lower right). The terrain is flat and lies ±3 m below the mean sea level. This region is dominated by agricultural crops and nominal field sizes are ≈80 ha. The major crops grown in area includes wheat, barley, potato, sugarbeet, and maize. Secondary crops include rapeseed, pea, onion, steam bean, and grass.

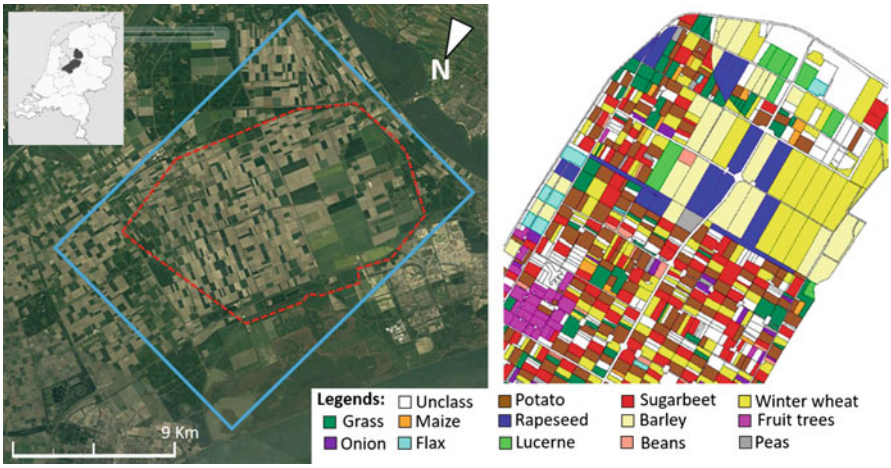

Fig. 1 The Flevoland test site location overlaid on Landsat-5 optical image. The extent of AIRSAR acquisition is presented in cyan rectangular box, and test site in red dashed line. A reference crop map indicates different agricultural crop parcels managed during the JPL-SAR experiment 1991

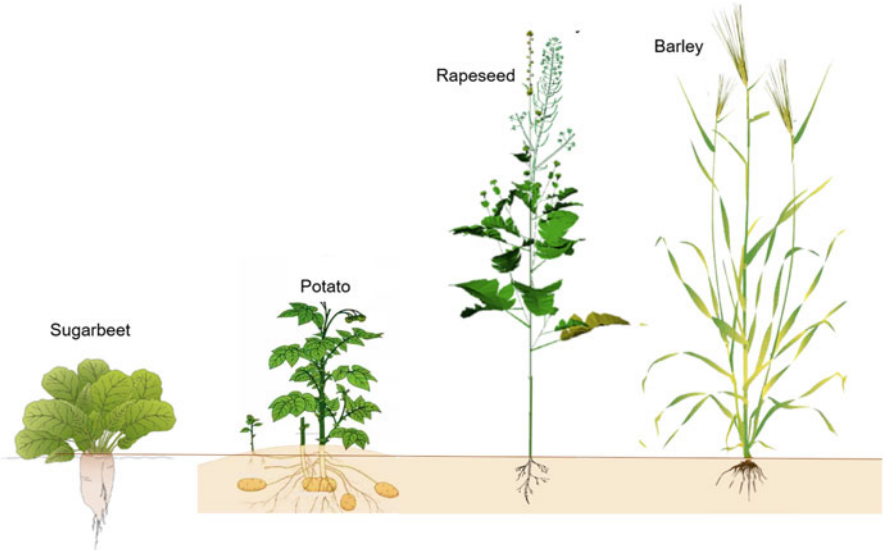

Fig. 2 Plant morphological structures for short-stem broad-leaf (sugarbeet and potato), and long-stem (rapeseed and barley) crops

For the analysis, we group these crops in two types: short-stem broad-leaf (SSBL), and long-stem (LS) (Fig. 2). In the long-stem category, barley and rapeseed were analyzed, while in the SSBL category, sugarbeet and potatoes were included. During the JPL-SAR experiment 1991, the Flevoland test site had 406, 317, 101, and 13 fields of potato, sugar beet, barley, and rapeseed, respectively [20, 54, 62].

We utilized the AIRSAR datasets [3] acquired during the campaign as part of the JPL-SAR experiment 1991. The acquisition of AIRSAR data (Process ID: cm3253, Flight-line: flevoland116-1.91109) coincided with the agricultural growing season in June. The acquisition of AIRSAR data was in multi-frequency (C-band: 5.7 cm, L-band: 25 cm, and P-band: 68 cm) and full-polarimetric mode. The nominal pixel spacing in range and azimuth was 6.66 m $\times$12.15 m. The AIRSAR data is provided in compressed Stokes product format.[1] We generate 3×3 covariance matrices for individual frequencies, i.e., C-, L-, and P-band from these products of AIRSAR data using PolSARPro toolbox. Other polarimetric features are subsequently generated from the elements of 3×3 covariance matrices. An overview of Pauli RGB images of these multi-frequency datasets over the Flevoland area is shown in Fig. 3.

[1] https://airsar.asf.alaska.edu/data/cm/cm3253/.

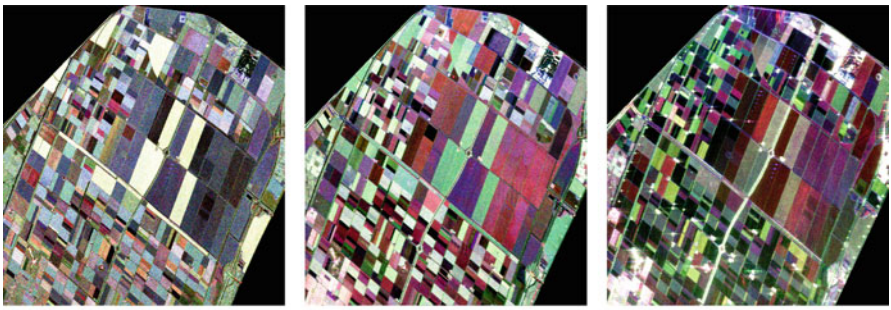

Fig. 3 Multi-frequency Pauli RGB images of the study area (Red=$|S_{\mathrm{HH}} - S_{\mathrm{VV}}|$, Green=$2|S_{\mathrm{HV}}|$, and Blue=$|S_{\mathrm{HH}} + S_{\mathrm{VV}}|$). These three colors are the magnitudes of the scattering matrix elements when they are expressed in the Pauli basis. (**a**) C-band. (**b**) L-band. (**c**) P-band

PolSAR Data Preprocessing Guidelines

SAR data processing guidelines in PolSARPro: https://github.com/dipankar05/springer-multifrequencySAR-crop/blob/main/PolSARpro_features_guide.pdf

In the H-V basis, we generated co-polarized phase (ϕ_{HH-VV}), co-polar coherence amplitude (ρ_{HHVV}), co- and cross-pol ratios ($\sigma^0_{HH}/\sigma^0_{VV}$, $\sigma^0_{HV}/\sigma^0_{HH}$, and $\sigma^0_{HV}/\sigma^0_{VV}$), and diagonal elements of the 3×3 covariance matrix. Subsequently, the covariance matrix in H-V basis is transformed to the circular R-L basis to obtain the $\sigma^0_{RR}/\sigma^0_{LL}$. Apart from these non-decomposition (ND) parameters, we derive 14 features from the target decomposition parameters [9, 60, 65], as presented in Table 1.

The training datasets for crop classification are generated using the reference map (Fig. 1) provided during the campaign and aptly used in literature [20, 62]. From these reference map, we generated training samples by drawing region of interest, which we kept at ≈15% sampling rate in this research. This selection of sampling rate is taken considering the stability in classification accuracies above 15%.

3 Methodology

3.1 Random Forest

Random Forests (RFs) are an ensemble learning technique for classification and regression which is constructed by several decision trees that are trained and their results are combined through a voting process by the majority of the individual decision trees [7]. The multiple decision trees of the RF are trained on a boot-

Table 1 SAR polarimetric decomposition (14) and non-decomposition (9) parameters used in this study

Decomposition parameters	Description
Touzi [60]	Touzi symmetric scattering type magnitude ($\alpha_{s_1}, \alpha_{s_2}$)
	Touzi symmetric scattering type phase (ϕ_{s_1}, ϕ_{s_2})
	Kennaugh-Huynen target helicity (τ_{m_1}, τ_{m_2})
Yamaguchi 4-component [65]	Odd-bounce scattering power (P_s), Double-bounce scattering power (P_d)
	Volume scattering power (P_v), Helix scattering power (P_c)
Cloude-Pottier [9]	Entropy (H), Anisotropy (A), Average target scattering mechanism (α); $Span = \sum_{i=1}^{3} \lambda_i$

Non-decomposition parameters	Description
Co-polarized phase	ϕ_{HH-VV}
Co-polar coherence amplitude	$\lvert\rho_{HHVV}\rvert$
Co-polarized and Cross-polarized Ratio	Co-polarized: $\sigma^0_{HH}/\sigma^0_{VV}$; Cross-polarized: $\sigma^0_{HV}/\sigma^0_{HH}$ and $\sigma^0_{HV}/\sigma^0_{VV}$ and $\sigma^0_{RR}/\sigma^0_{RL}$
Diagonal elements of the 3×3 covariance matrix	C_{11}, C_{22} and C_{33}

strapped sample of the original training data. At each node of every decision tree, one among a randomly selected subset of input parameters is chosen as the best split and subsequently used for node splitting [37]. Each tree uses only a portion of the input samples (typically two-third) for the training while the remaining roughly one-third (referred to as Out-Of-Bag (OOB)) of the samples are used to validate the accuracy of the prediction. In general, RF increases the diversity among the decision trees by randomly resampling the data with replacement and by randomly changing the parameter subsets for node splitting at each node of every decision tree.

3.2 Parameter Importance Evaluation

Parameter importance evaluation helps in identifying the most relevant parameters out of the total set for classification by ranking them in descending order of their importance. In RF, for every decision tree the misclassification rate is calculated from the OOB observations. The parameter whose importance is to be evaluated, is randomly permuted for the OOB observations, and then the modified OOB values are passed down the tree to get new predictions. This difference in the misclassification rate between the modified and the original OOB observations averaged over all trees, is the parameter importance measure which is used in this study [59]. This difference in classification accuracy before and after random permutation of the parameter whose importance is to be determined is the Mean

Decrease Accuracy (MDA) [49] measure used in this study. RF based parameter selection using this technique was studied in [2, 12, 21]. It is necessary to note that in this study the original MDA scores were normalized (the highest MDA score was set to 100 and the others were scaled accordingly) for the sake of comparison.

3.3 Partial Probability Plot

The RF is capable of identifying important parameters and generating partial dependence plots [18, 23] which may be used to establish relationships between the parameters and the predicted classes. The partial dependence plots provide an unique way to visualize the marginal effect of a parameter on the classification using RF. The partial dependence function is given as in (1) [18],

$$\widetilde{f}(x) = \frac{1}{n}\sum_{i=1}^{n} f(x, x_i c) \tag{1}$$

where x is the parameter for which partial dependence is sought, and $x_i c$ is the other parameters in the data.

$$f(x) = \log\ p_k(x) - \sum_j \log\ p_j(X)/K \tag{2}$$

The logits (i.e., log of fraction of votes) is the predicted classification function as given in (2). Here K is the number of classes and p_j is the proportion of votes for class j.

The partial dependency plots produced with probability distribution based on scaled margin distances are the partial probability plot used in this study. The partial probability plot provides a visual representation of the probability of occurrence of a class for each parameter over its entire dynamic range [5, 49]. By partialling out the average effect of all other parameters, we can analyze the influence of a given parameter on the probability of occurrence of the predicted class.

In this study, the partial probability plot of polarimetric parameters was useful for crop characterization and separation. For polarimetric parameters with diverse ranges, the partial probability plot helped to identify an optimal dynamic range [22] in which the probability of occurrence of "crop" class was $\geq$0.8. Identification of this range can be useful for crop characterization and separation. Mainly, the partial probability plots help to study the underlying physical scattering mechanisms associated with crops through their diverse optimal dynamic ranges.

3.4 Processing Steps for Parameter Selection and Classification Using RF

The schematic overview of the workflow used in this study is shown in Fig. 4.

The processing steps for multi-frequency crop classification in this study are as follows:

- Polarimetric target decomposition and non-decomposition parameters were generated from the coherency matrix and covariance matrix $\langle[\mathbf{T}]\rangle$ and $\langle[\mathbf{C}]\rangle$, which resulted in total 23 parameters.
- RF was created using 1000 decision trees and 23 parameters. It was decided to use 1000 decision trees since Breiman [7] suggested that as many trees as possible can be used in the RF ensemble since they do not overfit.
- Parameter selection and classification performed for each band (C-, L- & P-band) individually.
- The top 10 parameters with the highest MDA scores were chosen as the parameter subset in this study for multi-frequency crop classification.
- RF parameter ranking in co-ordination with partial probability plots were used to analyze separability and mixing among crop classes.

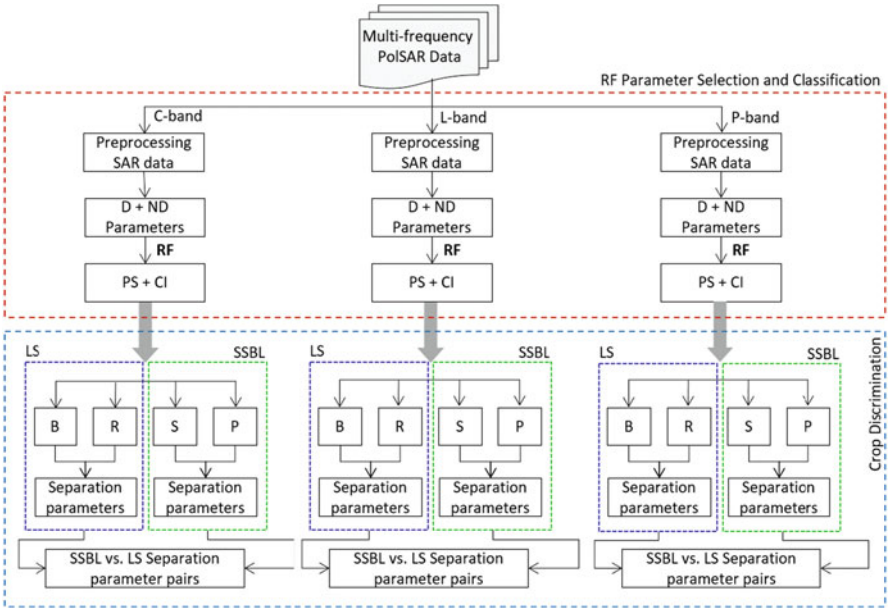

Fig. 4 Schematic workflow for multi-frequency crop classification and crop separability analysis using RF. D: Decomposition parameters, ND: Non-decomposition parameters, PS: Parameter Selection, Cl: Classification, SSBL: Short-stem broad-leaf crop, LS: Long-stem crop, B: Barley, R: Rapeseed, S: Sugarbeet, P: Potato

- In addition, we analyze separability of crop classes by measuring dissimilarity between partial probability plot curves using the Frèchet distance [1, 16]. The Frèchet distance closer to 0 indicates similarity between curves while closer to 1.0 indicates distinct curves.

RF Classification Code

RF Classification code along with partial probability plotting and Frèchet distance for R: https://github.com/dipankar05/springer-multifrequencySAR-crop/tree/main/Codes

4 Results and Discussion

Classification over the Flevoland area with the help of 23 polarimetric parameters was conducted. Out of this, only the top 10 were selected and subsequently used for classification with RF. These 10 parameters were used since it was observed that the Overall Accuracy (OA) does not change significantly beyond these parameters as shown in Fig. 5.

The number of training samples for each crop is given in Table 2. For ease of analysis, number of training and testing points of only 4 selected crops (2 in SSBL and 2 in LS categories) have been included out of the total 12 crop classes in the Flevoland study area.

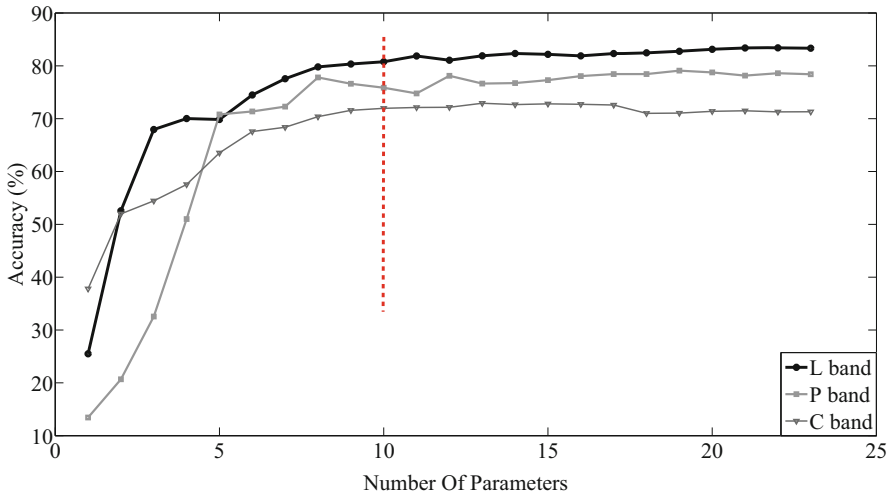

Fig. 5 Overall RF classification accuracy for number of parameters at multiple frequencies

Table 2 Flevoland: Number of training and test samples.

Crop	#Train	#Test1	#Test2
Barley	1100	600	592
Rapeseed	1115	563	571
Sugarbeet	2808	1342	1303
Potato	2357	1108	1119
Winter Wheat	1029	615	720
Lucerne	1516	636	688
Flax	1340	789	902
Beans	706	464	393
Fruit trees	1451	725	743
Grass	2281	1026	1251
Peas	855	439	409
Unclass	3009	1504	1314

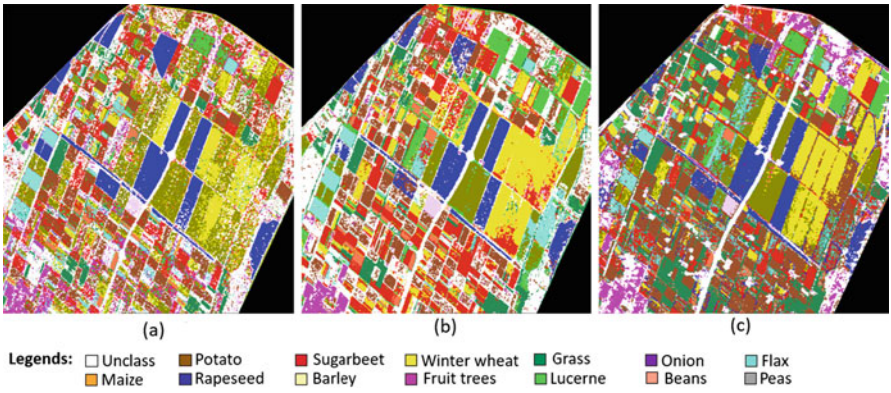

Fig. 6 RF classified images for C-, L-, and P-band over the Flevoland area. (**a**) C-band. (**b**) L-band. (**c**) P-band

The multi-frequency RF classified images are shown in Fig. 6. The overall classification accuracy for the multi-frequency crops are given in Table 3. In the following subsections we analyze the LS (barley and rapeseed) and SSBL (sugarbeet and potato) crops.

The number of test samples for each crop for the two sets is given in Table 2. The independence between two sets of randomly selected test samples was measured using the Wilcoxon signed-rank test [26, 63] using the sample median. The Wilcoxon signed-rank test evaluated the independence between these two sets of test samples to be $>90\%$ for all three bands (90.84%, 95.41%, and 96.36% for C-, L-, and P-band, respectively).

Table 3 RF Overall Accuracy using top 10 parameters

Class	C	L	P
Barley	66.81	91.73	86.18
Beans	78.45	86.85	80.39
Flax	92.65	99.75	90.75
Grass	67.84	43.18	63.06
Lucerne	47.64	99.69	83.49
Peas	71.99	97.77	80.52
Potatoes	84.32	95.42	94.57
Rapeseed	91.45	81.54	73.42
Winter wheat	77.03	73.13	44.27
Fruit trees	57.33	62.29	84.57
Sugarbeets	46.49	86.22	66.89
Unclass	22.39	63.27	98.53
Overall user accuracy (%)	71.95	80.77	75.85
Kappa	0.68	0.78	0.73

Table 4 RF classification accuracy for the two independent test samples

Band	Test1 (%)	Test2 (%)
C	71.31	68.08
L	83.33	83.30
P	78.41	77.14

Attention

The Wilcoxon signed-rank test [26, 63] was used in this study since it can be performed without assuming underlying distribution of the samples [40]; and we know that the polarimetric parameters in general for SAR data seldom follow normal distribution. The parameter median was calculated instead of mean since the mean of the parameter can be misleading when outliers are present in the data [35] which is possible for these kind of parameters.

The multi-frequency RF classification accuracy for the two test samples is given in Table 4. In addition, we provided the normalized MDA scores of top 10 parameters at C-, L-, and P-band for individual crops in Table 5, 6, 7, and 8.

4.1 Separation Among Long-Stem (LS) Crops

Stems of barley are long in length with thin diameter, and canopy consists of narrow leaves, while rapeseed plants have ramified stems with secondary and tertiary stems and pods. The RF parameter selection helped us to identify the important parameters for barley and rapeseed classification at different frequencies. The optimal dynamic range of these parameters were analyzed and the parameters which were used

Table 5 Normalized MDA scores of the top 10 parameters for barley classification

C-band	MDA scores	L-band	MDA scores	P-band	MDA scores
P_v	100	$\sigma^0_{HV}/\sigma^0_{HH}$	100	$\sigma^0_{HH}/\sigma^0_{VV}$	100
P_s	65.00	P_v	98.44	P_v	97.07
P_d	47.76	H	89.32	P_d	81.91
H	39.77	$\sigma^0_{HH}/\sigma^0_{VV}$	87.99	A	75.65
$\lvert\rho_{HHVV}\rvert$	38.45	P_d	83.26	$\sigma^0_{HV}/\sigma^0_{VV}$	71.40
$\sigma^0_{HH}/\sigma^0_{VV}$	34.33	α_{s_1}	72.97	P_s	65.33
P_c	32.52	Φ_{s_2}	69.29	Φ_{s_1}	62.44
α	29.71	P_s	68.78	$\sigma^0_{RR}/\sigma^0_{RL}$	60.91
Φ_{s_2}	27.92	$\lvert\rho_{HHVV}\rvert$	64.97	$\sigma^0_{HV}/\sigma^0_{HH}$	60.24
$\sigma^0_{HV}/\sigma^0_{HH}$	27.67	α_{s_2}	64.81	$SPAN$	56.81

Table 6 Normalized MDA scores of the top 10 parameters for rapeseed classification

C-band	MDA scores	L-band	MDA scores	P-band	MDA scores
P_v	100	P_c	100	P_v	100
$\sigma^0_{HV}/\sigma^0_{HH}$	53.07	$\sigma^0_{HV}/\sigma^0_{VV}$	74.41	P_c	83.93
$SPAN$	41.30	P_v	64.36	$\sigma^0_{HH}/\sigma^0_{VV}$	73.31
H	33.64	P_d	53.59	A	53.17
P_c	31.94	$\sigma^0_{HV}/\sigma^0_{HH}$	53.22	P_d	48.88
$\sigma^0_{HH}/\sigma^0_{VV}$	31.78	τ_{m_1}	48.50	Φ_{s_2}	46.70
$\sigma^0_{RR}/\sigma^0_{RL}$	31.49	Φ_{s_2}	47.58	Φ_{s_1}	45.71
α	30.94	Φ_{s_1}	44.35	$\lvert\rho_{HHVV}\rvert$	43.95
$\sigma^0_{HV}/\sigma^0_{VV}$	30.84	P_s	43.10	$\sigma^0_{HV}/\sigma^0_{HH}$	42.04
C_{22}	30.26	$\sigma^0_{HH}/\sigma^0_{VV}$	40.86	$\sigma^0_{HV}/\sigma^0_{VV}$	40.68

Table 7 Normalized MDA scores of the top 10 parameters for sugarbeet classification

C-band	MDA scores	L-band	MDA scores	P-band	MDA scores
P_v	100	$\sigma^0_{HV}/\sigma^0_{HH}$	100	τ_{m_2}	100
P_d	60.12	P_d	85.83	$\sigma^0_{HV}/\sigma^0_{HH}$	83.60
A	53.91	$\sigma^0_{HH}/\sigma^0_{VV}$	84.46	P_v	81.26
Φ_{s_2}	52.75	P_v	84.46	τ_{m_1}	72.49
τ_{m_1}	52.13	H	70.99	$\sigma^0_{HH}/\sigma^0_{VV}$	72.31
P_c	50.83	P_s	61.95	$\sigma^0_{HV}/\sigma^0_{VV}$	71.26
P_s	49.95	$\lvert\rho_{HHVV}\rvert$	58.80	P_d	67.16
$\sigma^0_{HH}/\sigma^0_{VV}$	47.94	Φ_{s_2}	58.75	A	67.09
$\sigma^0_{HV}/\sigma^0_{HH}$	46.84	$\sigma^0_{HV}/\sigma^0_{VV}$	57.42	α_{s_2}	63.76
$\sigma^0_{HV}/\sigma^0_{VV}$	38.88	α	56.23	P_s	61.14

to discriminate barley from rapeseed were identified to be P_v and P_c at C-band. The partial probability plots of P_v for barley and rapeseed given in Fig. 7a and b, respectively, show separation between them.

Table 8 Normalized MDA scores of the top 10 parameters for potato classification

C-band	MDA scores	L-band	MDA scores	P-band	MDA scores
$\lvert\rho_{HHVV}\rvert$	100	P_v	100	P_v	100
P_d	98.30	$\sigma^0_{HV}/\sigma^0_{VV}$	68.62	P_d	87.10
P_v	97.06	P_d	64.48	Φ_{s_2}	85.08
Φ_{s_2}	91.74	$\sigma^0_{HV}/\sigma^0_{HH}$	58.99	Φ_{s_1}	82.84
A	73.55	$\sigma^0_{HH}/\sigma^0_{VV}$	55.63	A	73.82
$\sigma^0_{HH}/\sigma^0_{VV}$	68.39	Φ_{s_1}	54.30	$\sigma^0_{HV}/\sigma^0_{VV}$	73.66
τ_{m_1}	57.96	Φ_{s_2}	53.57	$\sigma^0_{HH}/\sigma^0_{VV}$	73.54
P_c	55.55	P_s	52.91	$\sigma^0_{HV}/\sigma^0_{HH}$	71.59
$\sigma^0_{HV}/\sigma^0_{HH}$	52.90	τ_{m_1}	48.79	P_s	66.75
P_s	49.34	α	46.14	τ_{m_2}	63.48

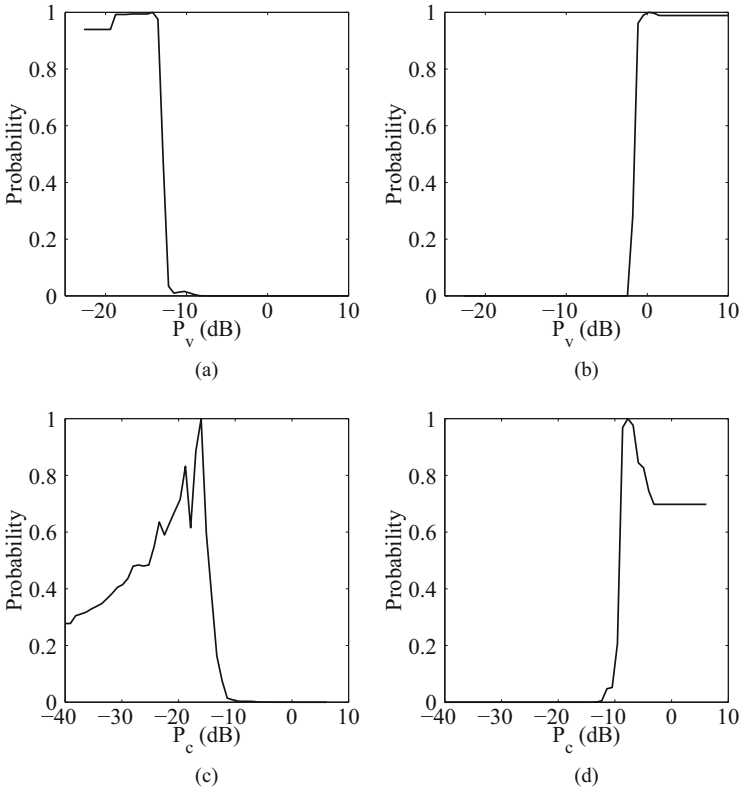

Fig. 7 Separation between barley and rapeseed using partial probability plots. (**a**) Barley C-band. (**b**) Rapeseed C-band. (**c**) Barley C-band. (**d**) Rapeseed C-band

The presence of secondary stems in rapeseed also gives rise to complex multiple or helical scattering thereby contributing to high P_c as compared to barley. The partial

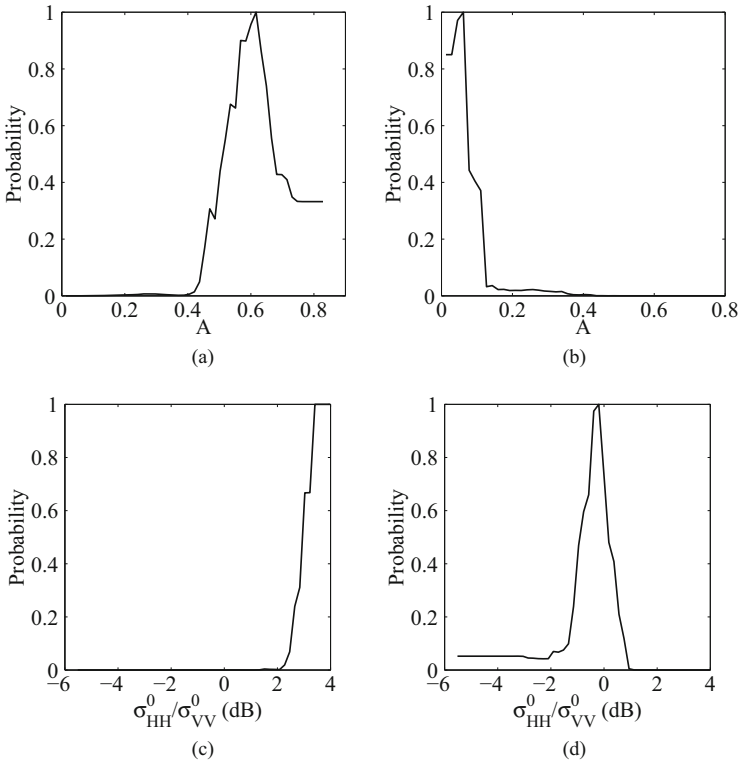

Fig. 8 separation between sugarbeet and potato using partial probability plots. (**a**) Sugarbeet L-band. (**b**) Potato L-band. (**c**) Sugarbeet L-band. (**d**) Potato L-band

probability plots of P_c for barley and rapeseed given in Fig. 7c and d, respectively, show separation between them.

Further, the Frèchet distance between the partial probability plots of P_v at C-band between barley and rapeseed was found to be 1.0, indicating high dissimilarity between the curves. Furthermore, the Frèchet distance between the partial probability plots of P_c at C-band between barley and rapeseed was found to be 0.99.

4.2 Separation Among Short-Stem Broad-Leaf (SSBL) Crops

The RF parameter selection and the optimal dynamic range evaluation using the partial probability plot was useful to discriminate sugarbeet from potatoes both being short-stem broad-leaf category. It was observed that sugarbeet and potatoes can be discriminated using A, and $\sigma^0_{HH}/\sigma^0_{VV}$ for L-band as shown in Fig. 8.

From the partial probability plots, the $\sigma^0_{HH}/\sigma^0_{VV}$ peak was observed to be more for sugarbeet as compared to potatoes at L-band as shown in Fig. 8c and d, respectively. Similar observation was reported by Skriver et al. [57]. This may be due to the relatively smooth surface scattering from sugarbeet compared to the rough surface scattering from potato. The anisotropy A for sugarbeet was reported to be higher than potatoes in L-band [51] which was also observed in our study as shown in Fig. 8a and b, respectively. Anisotropy can be effectively characterized for random scatterers for which $H \geq 0.7$ [32]. In our study for L-band, sugarbeet and potatoes were both observed to have $H \geq 0.7$. However, there was a difference in their anisotropy. Anisotropy is high when there is a big difference between the second and third scattering mechanisms. $A \approx 0$ implies that the second and the third dominant scattering mechanisms are almost the same. So in case of potato it seems that the second and third scattering mechanisms were equally dominant while for sugarbeet the third scattering mechanism (mostly noise) was non-existent as compared to the second dominant scattering mechanism.

The Frèchet distance between the partial probability plots of A at L-band for sugarbeet and potato was found to be 0.9. Additionally the Frèchet distance between the partial probability plots of $\sigma^0_{HH}/\sigma^0_{VV}$ at L-band for sugarbeet and potato was found to be 1.

4.3 Separation Between SSBL and LS Crops

Short-stem broad-leaf (SSBL) crops can be realized as canopy consisting of disc like scatterers. Unlike SSBL, the long-stem (LS) crops have predominantly cylindrical scatterers [20, 61]. It is important to identify polarimetric parameters which separate these two crop types. In this study we have determined a pair of polarimetric parameters based on the highest difference of MDA scores from the parameters selected by RF which best separate SSBL from LS crops. We first calculated the normalized MDA score difference between the same pair of parameters for two different crop types. The pair having the highest normalized MDA score difference between the two crops was selected for separation among the crop types. A few pairs of polarimetric parameters were thus identified which successfully separate SSBL from LS crops.

From Fig. 9a, it can be seen that for L-band, rapeseed (LS crop) and sugarbeet (SSBL crop) can be separated using $\sigma^0_{HH}/\sigma^0_{VV}$ and P_v and thus misclassification is avoided between them. The separation is about 4.0 dB for $\sigma^0_{HH}/\sigma^0_{VV}$ and about 10 dB for P_v. From Fig. 9b, it can be seen that for L-band, barley (LS crop) and potato (SSBL crop) can be separated successfully using the polarimetric parameter pair of $\sigma^0_{HV}/\sigma^0_{HH}$ and P_v. The separation is about 4.0 dB for $\sigma^0_{HV}/\sigma^0_{HH}$ and about 10.1 dB for P_v. As can be seen from Tables 5 and 7, the parameters $\sigma^0_{HH}/\sigma^0_{VV}$, and P_v are part of the top 10 parameters required for L-band classification of rapeseed and sugarbeet, respectively, thus validating the RF parameter ranking and

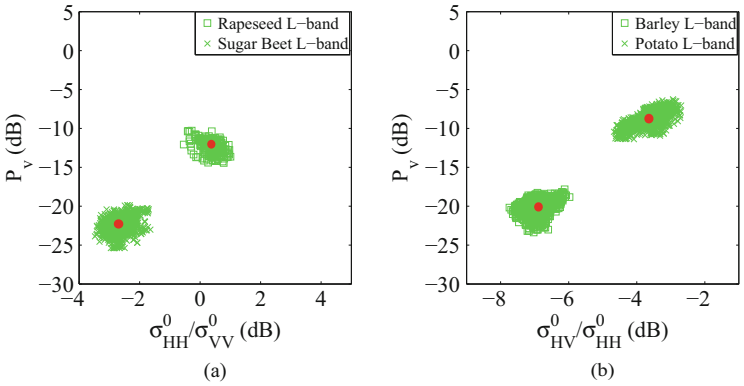

Fig. 9 Separation between small stem and broad-leaf crops at L-band. (**a**) Rapeseed-Sugarbeet. (**b**) Barley-Potato

its contribution in crop classification. Also $\sigma^0_{HV}/\sigma^0_{HH}$ and P_v are part of the top 10 parameters required for L-band classification of barley and sugarbeet, respectively, as seen from Tables 6 and 8.

From Fig. 10a, it can be seen that for P-band, rapeseed (LS crop) and sugarbeet (SSBL crop) crop can be separated using $\sigma^0_{HV}/\sigma^0_{HH}$ and P_d. The separation is about 2.5 dB for $\sigma^0_{HV}/\sigma^0_{HH}$ and about 6.0 dB for P_d. From Fig. 10b, it can be seen that for C-band, rapeseed (LS crop) and potato (BBSL crop) can be separated successfully using the polarimetric parameter pair of $\sigma^0_{HV}/\sigma^0_{HH}$ and P_c. The separation is about 2.5 dB for $\sigma^0_{HV}/\sigma^0_{HH}$ and about 4.0 dB for P_c. As can be seen from Tables 5 and 7, the parameters $\sigma^0_{HV}/\sigma^0_{VV}$, and P_d are part of the top 10 parameters required for P-band classification of rapeseed and sugarbeet, respectively, thus validating the RF parameter ranking and its contribution in crop classification. In fact they are amongst the top 5 ranked parameters for both crops. Also $\sigma^0_{HV}/\sigma^0_{HH}$ and P_c are part of the top 10 parameters required for C-band classification of rapeseed and potato, respectively, as seen from Tables 5 and 8.

4.4 Analyzing the Mixing Among Crop Classes

The RF classification accuracies were used to correlate the parameter ranking with the underlying physical scattering mechanism related to crop targets. RF based partial probability plots were used to study mixing among crop classes, since these plots give the marginal effect of the parameter on the classification accuracy. Analyzing partial probability plots to study mixing among crop classes helps us validate the RF parameter ranking. This is because the amount of mixing among crop classes is related to the more dominant parameters having similar partial

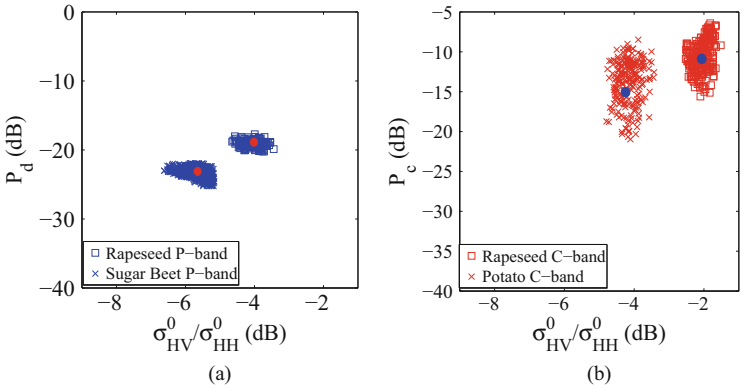

Fig. 10 Separation between small stem and broad-leaf crops at (**a**) P- and (**b**) C-band

Table 9 Confusion matrix for the four crop classes at C-band (%)

C	Barley	Rapeseed	Potato	Sugarbeet
Barley	84.54	0	0	1.27
Rapeseed	0	91.99	0	0
Potato	0	0	78.84	0
Sugarbeet	2.88	0.1	6.28	67.71

Table 10 Confusion matrix for the four crop classes at P-band (%)

P	Barley	Rapeseed	Potato	Sugar_beet
Barley	100	0	0	0
Rapeseed	0	76.91	0	0.28
Potato	0	18.34	99.63	0
Sugar_beet	0	0	0	59.21

probability plots. Distinct partial probability plots imply low to no mixing among crop classes.

In the confusion matrix (Table 9), it was observed that 6.28% of potato was misclassified as sugarbeet at C-band. The odd-bounce scattering power P_s (ranked 7 and 10 for sugarbeet and potato, respectively) had similar partial probability plots (Frèchet distance = 0.18) shown in Fig. 11a and b, respectively. This may be due to the fact that both potato and sugarbeet, being short-stem broad-leaf crops exhibit single bounce scattering from the wide leaf of the crop. Again from Table 10, in P-band, high mixing of 18.34% was observed among rapeseed and potato classes. The volume scattering power P_v is dominant for crops with ramified stems and was observed to be Rank 1 for both rapeseed and potato, respectively. P_v was observed to have relatively similar partial probability plots (Frèchet distance = 0.32) as shown in Fig. 12a and b, respectively.

In contrast to C and P-band, significant mixing was not observed among the four crops in L-band. This means the relevant parameters chosen by RF all have distinct partial probability plots at L-band. It was observed that barley and rapeseed crop classes did not have any intermixing among each other at all frequencies. Hence,

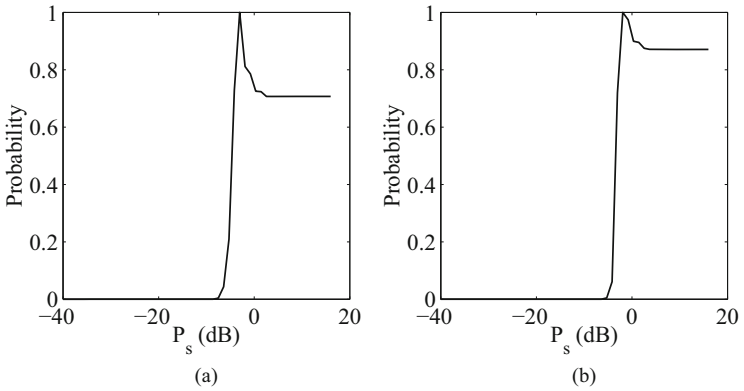

Fig. 11 Mixing among sugarbeet and potato classes at C-band. (**a**) Sugarbeet. (**b**) Potato

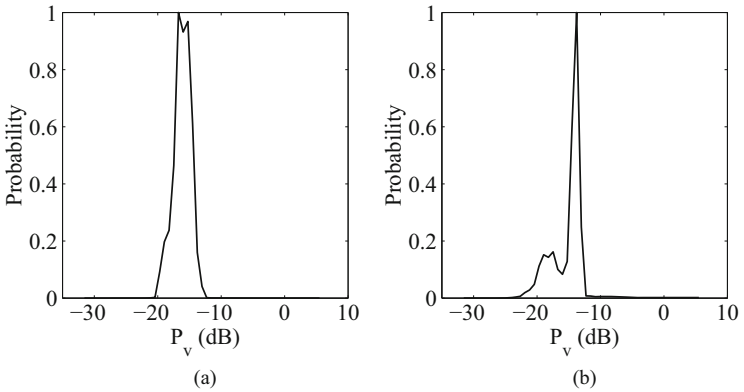

Fig. 12 Mixing among rapeseed and potato classes at P-band. (**a**) Rapeseed. (**b**) Potato

it is interesting to note that the top parameters selected by RF have distinct partial probability plots for barley and rapeseed at all frequencies. The partial probability plots of $\sigma^0_{HV}/\sigma^0_{HH}$ (ranked 1 and 5 for barley and rapeseed, respectively) at L-band is shown in Fig. 13a and b. The Frèchet distance between them was observed to be 0.97 indicating distinct plots. It is to be noted that the confusion matrix given in Tables 9 and 10 do not sum up to 100%, since only classification accuracies of 4 selected crops have been included out of the total 12 crop classes in the Flevoland study area.

Some notable insights from the above study:

- When top ranked parameters of different crops have similar partial probability plots, the crop classes can be easily mixed.
- Mixing among crop classes reduces as the rankings get lowered for parameters with similar partial probability plots. For instance, 18.34% mixing was observed

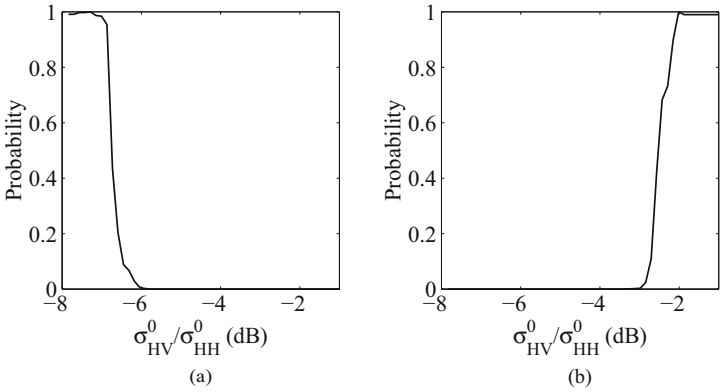

Fig. 13 Distinct partial probability plots of selected parameters for barley and rapeseed (L-band). (**a**) Barley. (**b**) Rapeseed

among crops classes for top ranked parameters (rank 1–3) while only 6.28% mixing for bottom ranked parameters (rank 7–10).

- Crop classes which do not mix, their top ranked parameters mostly have distinct partial probability plots.

5 Summary

In this study we utilized polarimetric target decomposition and non-decomposition parameters for crop analysis. It was observed that the model-based decomposition powers along with the ratio of the backscattering coefficients were important for crop classification. Moreover the Eigenvalue/Eigenvector based decomposition parameters were useful for critical analysis of crops in some cases. It was observed that similar crop types have different scattering properties which was evident from the partial probability plots of the important polarimetric parameters. The parameter selection by RF and the evaluated normalized MDA scores for multi-frequency data was thus useful for crop analysis. Separation between Long-stem and short-stem broad-leaf crops at different frequencies was made possible using a pair of polarimetric parameters having the highest normalized MDA score difference between the crop types. It was seen that the crops which were separated physically by the polarimetric parameter ranges were also the ones having the highest difference between their normalized MDA scores. This was helpful in validating the RF parameter ranking at multiple frequencies.

This study can be extended by incorporating parameters from multiple sources, for example: Leaf Area Index (LAI), Normalized Difference Vegetation Index (NDVI), soil moisture, temperature, etc., in addition to polarimetric parameters. The ranking of these parameters from multiple sources can be useful for diverse

crop analysis studies. The partial probability plots which evaluate optimal dynamic ranges can be useful for further analysis like crop yield, annual crop growth monitoring, etc. Multi-temporal analysis in addition to multi-frequency can be of an added advantage for crop studies. Evaluation of optimal dynamic ranges for crop parameters over the entire growth stage for multi-temporal datasets will be very useful for agriculture studies like crop planning and harvest.

Acknowledgments The authors would like to thank the NASA/JPL for providing AIRSAR data products. Authors acknowledge the GEO-AWS Earth Observation Cloud Credits Program, which supported the computation on AWS cloud platform through the project: "AWS4AgriSAR-Crop inventory mapping from SAR data on cloud computing platform."

References

1. Alt H, Godau M (1995) Computing the Fréchet distance between two polygonal curves. International Journal of Computational Geometry & Applications 5(01n02):75–91
2. Archer KJ, Kimes RV (2008) Empirical characterization of random forest variable importance measures. Computational Statistics & Data Analysis 52(4):2249–2260
3. ASF (Retrieved from ASF DAAC 25 December 2020) Dataset: AIRSAR, NASA 1991. https://asf.alaska.edu/
4. Bargiel D (2017) A new method for crop classification combining time series of radar images and crop phenology information. Remote sensing of environment 198:369–383
5. Baruch-Mordo S, Evans JS, Severson JP, Naugle DE, Maestas JD, Kiesecker JM, Falkowski MJ, Hagen CA, Reese KP (2013) Saving sage-grouse from the trees: A proactive solution to reducing a key threat to a candidate species. Biological Conservation 167(0):233–241, https://doi.org/10.1016/j.biocon.2013.08.017, http://www.sciencedirect.com/science/article/pii/S0006320713002917
6. Blaes X, Vanhalle L, Defourny P (2005) Efficiency of crop identification based on optical and SAR image time series. Remote sensing of environment 96(3):352–365
7. Breiman L (2001) Random forests. Machine learning 45(1):5–32
8. Chen K, Huang W, Tsay D, Amar F (1996) Classification of multifrequency polarimetric SAR imagery using a dynamic learning neural network. Geoscience and Remote Sensing, IEEE Transactions on 34(3):814–820
9. Cloude S, Pottier E (1997) An entropy based classification scheme for land applications of polarimetric SAR. Geoscience and Remote Sensing, IEEE Transactions on 35(1):68–78, https://doi.org/10.1109/36.551935
10. Deschamps B, McNairn H, Shang J, Jiao X (2012) Towards operational radar-only crop type classification: comparison of a traditional decision tree with a random forest classifier. Canadian Journal of Remote Sensing 38(1):60–68
11. Dey S, Mandal D, Robertson LD, Banerjee B, Kumar V, McNairn H, Bhattacharya A, Rao Y (2020) In-season crop classification using elements of the Kennaugh matrix derived from polarimetric radarsat-2 SAR data. International Journal of Applied Earth Observation and Geoinformation 88:102059
12. Díaz-Uriarte R, De Andres SA (2006) Gene selection and classification of microarray data using random forest. BMC bioinformatics 7(1):3
13. Dingle Robertson L, M Davidson A, McNairn H, Hosseini M, Mitchell S, de Abelleyra D, Verón S, Le Maire G, Plannells M, Valero S, et al. (2020) C-band synthetic aperture radar (sar) imagery for the classification of diverse cropping systems. International Journal of Remote Sensing 41(24):9628–9649

14. Ferrazzoli P, Guerriero L, Schiavon G (1999) Experimental and model investigation on radar classification capability. Geoscience and Remote Sensing, IEEE Transactions on 37(2):960–968
15. Foody G, McCulloch M, Yates W (1994) Crop classification from c-band polarimetric radar data. International Journal of Remote Sensing 15(14):2871–2885
16. Fréchet MM (1906) Sur quelques points du calcul fonctionnel. Rendiconti del Circolo Matematico di Palermo (1884–1940) 22(1):1–72
17. Freeman A, Villasenor J, Klein J, Hoogeboom P, Groot J (1994) On the use of multi-frequency and polarimetric radar backscatter features for classification of agricultural crops. International Journal of Remote Sensing 15(9):1799–1812
18. Friedman JH (2001) Greedy function approximation: A gradient boosting machine. The Annals of Statistics 29(5):pp. 1189–1232, http://www.jstor.org/stable/2699986
19. Gonzalez-Sampedro M, Le Toan T, Davidson M, Moreno J (2002) Assessment of crop discrimination using multi-site databases. EUROPEAN SPACE AGENCY-PUBLICATIONS-ESA SP 475:63–68
20. González Sanpedro M, et al. (2008) Optical and radar remote sensing applied to agricultural areas in Europe. Universitat de València
21. Hariharan S, Tirodkar S, De S, Bhattacharya A (2014) Variable importance and random forest classification using radarsat-2 PolSAR data. In: Geoscience and Remote Sensing Symposium (IGARSS), 2014 IEEE International, pp 1210–1213, https://doi.org/10.1109/IGARSS.2014.6946649
22. Hariharan S, Mandal D, Tirodkar S, Kumar V, Bhattacharya A, Lopez-Sanchez JM (2018) A novel phenology based feature subset selection technique using random forest for multitemporal PolSAR crop classification. IEEE Journal of Selected Topics in Applied Earth Observations and Remote Sensing 11(11):4244–4258
23. Hastie T, Tibshirani R, Friedman J, Franklin J (2005) The elements of statistical learning: data mining, inference and prediction. The Mathematical Intelligencer 27(2):83–85
24. Hoekman DH, Vissers MA (2003) A new polarimetric classification approach evaluated for agricultural crops. Geoscience and Remote Sensing, IEEE Transactions on 41(12):2881–2889
25. Hoekman DH, Vissers MA, Tran TN (2011) Unsupervised full-polarimetric SAR data segmentation as a tool for classification of agricultural areas. Selected Topics in Applied Earth Observations and Remote Sensing, IEEE Journal of 4(2):402–411
26. Hollander M, Wolfe DA, Chicken E (2013) Nonparametric statistical methods. John Wiley & Sons
27. Inoue Y, Kurosu T, Maeno H, Uratsuka S, Kozu T, Dabrowska-Zielinska K, Qi J (2002) Season-long daily measurements of multifrequency (Ka, Ku, X, C, and L) and full-polarization backscatter signatures over paddy rice field and their relationship with biological variables. Remote Sensing of Environment 81(2–3):194–204
28. Jia M, Tong L, Zhang Y, Chen Y (2013) Multitemporal radar backscattering measurement of wheat fields using multifrequency (l, s, c, and x) and full-polarization. Radio Science 48(5):471–481
29. Jiao X, Kovacs JM, Shang J, McNairn H, Walters D, Ma B, Geng X (2014) Object-oriented crop mapping and monitoring using multi-temporal polarimetric radarsat-2 data. ISPRS Journal of Photogrammetry and Remote Sensing 96:38–46
30. Kumar V, Rao YS, Bhattacharya A, Cloude SR (2019) Classification assessment of real versus simulated compact and quad-pol modes of alos-2. IEEE Geoscience and Remote Sensing Letters 16(9):1497–1501
31. Kussul N, Mykola L, Shelestov A, Skakun S (2018) Crop inventory at regional scale in Ukraine: developing in season and end of season crop maps with multi-temporal optical and SAR satellite imagery. European Journal of Remote Sensing 51(1):627–636
32. Lee JS, Pottier E (2009) Polarimetric radar imaging: from basics to applications. CRC Press
33. Lee JS, Grunes MR, Pottier E (2001) Quantitative comparison of classification capability: fully polarimetric versus dual and single-polarization SAR. Geoscience and Remote Sensing, IEEE Transactions on 39(11):2343–2351

34. Lemoine G, De Grandi G, Sieber A (1994) Polarimetric contrast classification of agricultural fields using maestro 1 AIRSAR data. International journal of remote sensing 15(14):2851–2869
35. Leys C, Ley C, Klein O, Bernard P, Licata L (2013) Detecting outliers: do not use standard deviation around the mean, use absolute deviation around the median. Journal of Experimental Social Psychology 49(4):764–766
36. Li H, Zhang C, Zhang S, Atkinson PM (2020) Crop classification from full-year fully-polarimetric l-band UAVSAR time-series using the random forest algorithm. International Journal of Applied Earth Observation and Geoinformation 87:102032
37. Liaw A, Wiener M (2002) Classification and regression by randomForest. R news 2(3):18–22
38. Loosvelt L, Peters J, Skriver H, De Baets B, Verhoest NE (2012) Impact of reducing polarimetric SAR input on the uncertainty of crop classifications based on the random forests algorithm. Geoscience and Remote Sensing, IEEE Transactions on 50(10):4185–4200
39. Löw F, Michel U, Dech S, Conrad C (2013) Impact of feature selection on the accuracy and spatial uncertainty of per-field crop classification using support vector machines. ISPRS Journal of Photogrammetry and Remote Sensing 85:102–119
40. Lumley T, Diehr P, Emerson S, Chen L (2002) The importance of the normality assumption in large public health data sets. Annual review of public health 23(1):151–169
41. Macelloni G, Paloscia S, Pampaloni P, Marliani F, Gai M (2001) The relationship between the backscattering coefficient and the biomass of narrow and broad leaf crops. Geoscience and Remote Sensing, IEEE Transactions on 39(4):873–884
42. Mahdianpari M, Mohammadimanesh F, McNairn H, Davidson A, Rezaee M, Salehi B, Homayouni S (2019) Mid-season crop classification using dual-, compact-, and full-polarization in preparation for the Radarsat constellation mission (RCM). Remote Sensing 11(13):1582
43. Mandal D, Kumar V, Rao YS (2020) An assessment of temporal RADARSAT-2 SAR data for crop classification using KPCA based support vector machine. Geocarto International pp 1–13
44. Mandal D, Bhattacharya A, Rao YS (2021) Radar Remote Sensing for Crop Biophysical Parameter Estimation. Springer
45. McNairn H, Brisco B (2004) The application of c-band polarimetric SAR for agriculture: a review. Canadian Journal of Remote Sensing 30(3):525–542
46. McNairn H, Duguay C, Brisco B, Pultz T (2002) The effect of soil and crop residue characteristics on polarimetric radar response. Remote sensing of environment 80(2):308–320
47. McNairn H, Shang J, Champagne C, Jiao X (2009) TerraSAR-x and radarsat-2 for crop classification and acreage estimation. In: Geoscience and Remote Sensing Symposium, 2009 IEEE International, IGARSS 2009, IEEE, vol 2, pp II–898
48. McNairn H, Shang J, Jiao X, Champagne C (2009) The contribution of ALOS PALSAR multipolarization and polarimetric data to crop classification. Geoscience and Remote Sensing, IEEE Transactions on 47(12):3981–3992
49. R Core Team (2013) R: A Language and Environment for Statistical Computing. R Foundation for Statistical Computing, Vienna, Austria, http://www.R-project.org/, ISBN 3-900051-07-0
50. Rao K, Rao Y, Wang J (1995) Frequency dependence of polarization phase difference. International Journal of Remote Sensing 16(18):3605–3617
51. Riedel T, Liebeskind P, Schmullius C (2002) Seasonal and diurnal changes of polarimetric parameters from crops derived by the Cloude decomposition theorem at l-band. In: Geoscience and Remote Sensing Symposium, 2002. IGARSS'02. 2002 IEEE International, IEEE, vol 5, pp 2714–2716
52. Robertson LD, Davidson A, McNairn H, Hosseini M, Mitchell S (2019) Assessment of multi-frequency SAR for crop type classification and mapping. In: IGARSS 2019–2019 IEEE International Geoscience and Remote Sensing Symposium, IEEE, pp 489–492
53. Saich P, Borgeaud M (2000) Interpreting ERS SAR signatures of agricultural crops in Flevoland, 1993–1996. Geoscience and Remote Sensing, IEEE Transactions on 38(2):651–657
54. Schotten C, Van Rooy W, Janssen L (1995) Assessment of the capabilities of multi-temporal ers-1 SAR data to discriminate between agricultural crops. International Journal of Remote Sensing 16(14):2619–2637

55. Skriver H (2012) Crop classification by multitemporal c-and l-band single-and dual-polarization and fully polarimetric SAR. Geoscience and Remote Sensing, IEEE Transactions on 50(6):2138–2149
56. Skriver H, Svendsen MT, Nielsen F, Thomsen A (1999) Crop classification by polarimetric SAR. In: Geoscience and Remote Sensing Symposium, 1999. IGARSS'99 Proceedings. IEEE 1999 International, IEEE, vol 4, pp 2333–2335
57. Skriver H, Svendsen MT, Thomsen AG (1999) Multitemporal c-and l-band polarimetric signatures of crops. Geoscience and Remote Sensing, IEEE Transactions on 37(5):2413–2429
58. Sonobe R, Tani H, Wang X, Kobayashi N, Shimamura H (2014) Random forest classification of crop type using multi-temporal TerraSAR-x dual-polarimetric data. Remote Sensing Letters 5(2):157–164
59. Strobl C, Zeileis A (2008) Danger: High power!? Exploring the statistical properties of a test for random forest variable importance. http://nbn-resolving.de/urn/resolver.pl?urn=nbn:de:bvb:19-epub-2111-8
60. Touzi R (2007) Target scattering decomposition in terms of roll-invariant target parameters. Geoscience and Remote Sensing, IEEE Transactions on 45(1):73–84, https://doi.org/10.1109/TGRS.2006.886176
61. Ulaby FT, Dobson MC (1989) Handbook of radar scattering statistics for terrain. ARTECH HOUSE, 685 CANTON STREET, NORWOOD, MA 02062(USA), 1989, 500
62. Vissers M, van der Sanden J (1992) Groundtruth collection for the JPL-SAR and ERS-1 campaign in Flevoland and the Veluwe (NL) 1991. Tech. Rep. BCRS 92–26, Netherlands Remote Sensing Board
63. Wilcoxon F (1945) Individual comparisons by ranking methods. Biometrics bulletin pp 80–83
64. Xie Q, Wang J, Liao C, Shang J, Lopez-Sanchez JM, Fu H, Liu X (2019) On the use of Neumann decomposition for crop classification using multi-temporal radarsat-2 polarimetric SAR data. Remote Sensing 11(7):776
65. Yamaguchi Y, Moriyama T, Ishido M, Yamada H (2005) Four-component scattering model for polarimetric SAR image decomposition. Geoscience and Remote Sensing, IEEE Transactions on 43(8):1699–1706, https://doi.org/10.1109/TGRS.2005.852084